International Journal of Pharmaceutics 391 (2010) 260–266

Contents lists available at ScienceDirect

International Journal of Pharmaceutics

journal homepage: www.elsevier.com/locate/ijpharm

Pharmaceutical Nanotechnology

Stearic acid grafted chitosan oligosaccharide micelle as a promising vector for gene delivery system: Factors affecting the complexation

Yong-Zhong Du[a], Ping Lu[a,b], Jian-Ping Zhou[b,*], Hong Yuan[a], Fu-Qiang Hu[a,*]

[a] College of Pharmaceutical Science, Zhejiang University, 388 Yuhangtang Road, Hangzhou 310058, PR China
[b] Department of Pharmaceutics, China Pharmaceutical University, 24 Tongjiaxiang Road, Nanjing 210009, PR China

ARTICLE INFO

Article history:
Received 9 November 2009
Received in revised form 8 January 2010
Accepted 10 February 2010
Available online 17 February 2010

Keywords:
Chitosan oligosaccharide
Stearic acid
Cationic micelles
Gene delivery vector
Complexation
Stability

ABSTRACT

Stearic acid (SA) grafted chitosan oligosaccharide (CSO-SA) with different molecular weight of chitosan oligosaccharide (CSO) and graft ratio of stearic acid were synthesized by coupling reaction of SA and CSO. The cationic polymeric micelles of CSO-SA via self-assemble formed and used for gene delivery of fish sperm DNA. Factors affecting complexation and stability of the complexes of CSO-SA micelles and DNA were investigated. The results indicated that pKa of CSO-SA with 3 kDa of CSO decreased from 8.16 to 6.02 as the substitution degree of amino groups of CSO in CSO-SA increased from 9.79% to 63.41%, whereas the molecular weight (M_W) of CSO less affected the pKa. As for the stability of complexes, ethidium bromide assay data demonstrated that the complexes consisting of CSO-SA with lower amino substitution degree or smaller molecular weight of CSO were more stable than that with the higher amino substitution degree or molecular weight of CSO. The results also presented that the low pH and ionic strength environment were in favor for the stability of complexes.

1. Introduction

Effort had been made to evaluate the potentials and benefits of synthetic gene vector, such as liposome, dendrimer and polycation (Wasungu and Hoekstra, 2006; Zhang et al., 2007; Kim et al., 2009), as alternatives to viral vector for gene delivery. Therein, polycation attracted a great deal of attention, because of their low immunogenicity, cationic properties, ease to preparation and structure modification. Cationic polycation can complex with anionic DNA through electrostatic interaction in normal condition without special treatment, avoiding the possible damage to DNA. However, polycation was far away from a perfect gene vector such as lacking of degradability, low biocompatibility, and in particular, low transfection efficiency compared with viral vector.

Chitosan, a natural cationic polysaccharide had shown excel in gene delivery. A majority of work had been done on chitosan (Lee et al., 1998; MacLaughlin et al., 1998; Richardson et al., 1999) and it was found that chitosan was a kind of biocompatible, biodegradable, and low toxic material having cationic potential in physical condition, and had primary amino groups that allowed being further modified (Kim et al., 2007). However, chitosan had several disadvantages, which handicapped its successful application in gene delivery. One of the major disadvantages was the low transfection efficiency. The transfection efficiency in vitro was reported ranging from 0.05% to 12.1% (Huang et al., 2005), much lower than that of Lipofectamine™ 2000 (about 20%). The other disadvantages included the solubility problem and lacking of cell specificity. Chemical modification of chitosan was a feasible way to overcome those disadvantages, making it more suitable as gene vector. The reported chemical modification can be classified as potential modification, hydrophilic modification, hydrophobic modification, pH-sensitive modification, temperature-sensitive modification and special ligand modification (Kim et al., 2007). Jiang et al. (2007) and Kim et al. (2003) had confirmed the enhancement of transfection efficiency after chemical modification of chitosan. Low molecular weight chitosan attracted great attention because of good solubility in physiological condition, higher gene transfection (Köping-Höggård et al., 2004) and more efficient enzymatic protection (Richardson et al., 1999). Those phenomenons can be explained that molecular weight may influence the stability of complexes, the efficiency of cellular uptake, or the dissociation rate of DNA from complexes after endocytosis (Liu and Yao, 2002).

Stearic acid grafted chitosan oligosaccharide (CSO-SA) is a kind of hydrophobic modification of chitosan oligosaccharide developed by our lab (Hu et al., 2006a). The CSO-SA could form micelles in the aqueous medium, and the CSO-SA micelles could be rapidly internalized into cancer cells (You et al., 2007). Besides having the merits of chitosan, such as biocompatibility, biodegradability, CSO-SA also owns the characterization of good solubility in distilled water, narrow size distribution, reduced cell toxicity and suitable positive

* Corresponding authors. Tel.: +86 571 88208439; fax: +86 571 88208439.
E-mail addresses: jpzhoucpu@126.com (J.-P. Zhou), hufq@zju.edu.cn (F.-Q. Hu).

0378-5173/$ – see front matter © 2010 Elsevier B.V. All rights reserved.
doi:10.1016/j.ijpharm.2010.02.017

charge (Hu et al., 2006b), all of which make it as a promising gene vector candidate.

There were demonstrated that the gene transfection efficiencies had relationship with the N/P ratio, size, stability, ability of cellular uptake of complexes, and the dissociation rate of DNA from complexes after endocytosis (Wetering et al., 1997; Dokka et al., 2000; Prabha et al., 2002). Among those, size and stability of complexes are the two major parameters to obtain efficient transfection. The size of chitosan nanoparticles dictated it permeabilizing on the cell membrane (Hu et al., 2006a) and the complexes with smaller size had advantages in entering the cells through endocytosis, therefore increasing the transfection rate (Mansouri et al., 2004). It was found that the nanoparticles with diameter 70 ± 2 nm exhibited 27-fold higher transfection efficiency in CSO-7 cell line than that with bigger diameter (202 ± 9 nm) (Prabha et al., 2002). The binding affinity of polycation with DNA in response to the addition of salt and pH change was determined by ethidium bromide displacement assay, which was a conventional way of monitoring the interaction of polyelectrolyte. High binding affinity leaded to DNA condensation, then to high stability and ultimately to high transfection efficiency (Geall et al., 1999).

The aim of present study is to gain insight into formulation parameters such as ionic strength, pH, N/P ratio (nitrogen/phosphate ratio) and the properties of CSO-SA (molecular weight of CSO-SA, amino substitution degree, pKa) which have impact on the complexation and stability of complexes. Data obtained in present work tends to provide the guideline in design of complexes with high stability and transfection efficiency, which are particularly important to be a gene delivery system using modified chitosan.

2. Materials and methods

2.1. Materials

Chitosan (M_W: 450.0 kDa, Deacetylation Degree: 95%) was obtained from Yuhuan Marine Biochemistry Co., Ltd. (Zhejiang, China). Chitosanase was purchased from Chemical Industries Co., Ltd. (Japan). Stearic acid was purchased from Shanghai Chemical Reagent Co., Ltd. (China). 1-Ethyl-3-(3-dimethylaminepropyl) carbodiimide (EDC), 2,4,6-trinitrobenzene sulfonic acid (TNBS) and ethidium bromide (EtBr) was purchased from Sigma (St. Louis, USA). Sodium hydroxide (NaOH) and hydrochloride (HCl) were purchased from Hangzhou chemical reagent Co., Ltd. (Zhejiang, China). Fish sperm DNA was purchased from Sangon Biological Engineering Technology & Service Co., Ltd. (Shanghai China). Other reagents used in the experiment were analytical grade.

2.2. Synthesis of CSO-SA

Chitosan oligosaccharide (CSO) was prepared by enzymatic hydrolysis of chitosan (M_W: 450 kDa, deaceylation degree: 95%) (Hu et al., 2006b). The hydrolysis process was monitored by gel permeation chromatography (GPC) and terminated when desirable molecular weight was obtained. The reactant was further purified by ultra-filtration to obtain the product with narrow molecular weight distribution. Stearic acid (SA) was then coupled with chitosan oligosaccharide via reaction of carboxyl groups of SA with primary amino groups of CSO catalyzed by EDC. Briefly, CSO (1 g) was dissolved in 200 mL super-purified water, and SA (the amount of SA was varied with the different type of CSO-SA) and EDC was dissolved in 100 mL ethanol. The carboxyl groups of SA were activated by EDC, which was 10-fold molar excess over SA. The activated SA was added into CSO solution and allowed to react with 400 rpm for 24 h at 60 °C water bath. The final reactant was dialyzed by employing dialysis membrane (M_W: 3 kDa, Spectrum Laboratories, Laguna Hills, CA) against super-purified water for 72 h in order to remove the by-product completely. The dialyzed product was then lyophilized.

2.3. Determination of critical micelle concentration (CMC)

Pyrene fluorescence method was employed for CMC determination of CSO-SA. First of all, pyrene stock solution was prepared by dissolving 6 mg pyrene in 50 mL acetone. The pyrene stock solution was further diluted with acetone for 100 times. 0.5 mL aliquots of pyrene solution with concentration of 0.0012 mg/mL were transferred precisely into test tubes and the solvent was evaporated in dark at 50 °C. 5 mL polymer solution with concentration range 1.25 mg/mL to 10^{-4} mg/mL was added to test tubes and the final concentration of pyrene in mixtures was controlled at 6×10^{-7} M. The emission spectra of mixture was measured by using fluorometer (F-2500, HITACHI Co., Japan). The excitation wavelength was 337 nm. The slit openings of excitation and emission were set at 10 nm and 2.5 nm, respectively.

2.4. Preparation of CSO-SA/DNA complexes

Briefly, commercial fish sperm DNA (5 mg/mL) was diluted with super-purified water to give a concentration of 1 mg/mL. The CSO-SA/DNA charge ratio was expressed as molar ratio of the primary amino groups of CSO-SA to those of the phosphate groups of DNA (N/P ratio). The complexes with different N/P ratio were then prepared by dropwise addition of DNA solution into CSO-SA solution with concentration of 1 mg/mL at ambient temperature, and following gentle magnetic stirring for 5 min.

2.5. Size and zeta potential determination

The sizes and zeta potentials of CSO-SA micelles and CSO-SA/DNA complexes were measured by Dynamic Light Scattering (Zetasizer $3000HS_A$, Malvern Instruments Ltd., UK). Sizes were presented in this section is *Z*-average diameter value. Each sample determination was done in triplicate.

2.6. TNBS assay

TNBS assay was employed to determine quantitatively the substitution degree (SD) of amino groups in CSO-SA. 10 mg of CSO-SA was dissolved in 10 mL of super-purified water. Then, 300 μL of 1 mg/mL CSO-SA solution was mixed with 2 mL of sodium hydrogen carbonate (4%, w/v) and 2 mL of TNBS solution (0.1%, w/v), which was incubated in water bath for 2 h at 37 °C. The UV absorbance at 344 nm of the product against a blank prepared with super-purified water, sodium hydrogen carbonate solution and TNBS solution under same process was determined by UV spectrophotometer (TU-1800PC, Beijing Purkinje General Instrument Co., Ltd., China) after 2 mL of hydrochloric acid was added. SD of CSO-SA was calculated from the UV absorbance of CSO-SA and unmodified CSO.

2.7. Potentiometric measurement

CSO-SA (10 mg) was dissolved in 20 mL super-purified water to prepare CSO-SA solution with concentration of 0.5 mg/mL. Equal aliquots of NaOH solution (0.01 M) was titrated precisely into CSO-SA solution by using pipette with stirring at rate of 400 rpm during the addition. pH was measured by pH meter (320pH meter, Metter Toledo, USA) after titration equilibrium was achieved.

2.8. Ethidium bromide displacement assay

Ethidium bromide displacement assay can be characterized the binding ability of CSO-SA with DNA. 20 μL of DNA solution (5 mg/mL) was diluted to 5 mL with sodium chloride solution (10 mM). The diluted DNA (20 μg/mL) solution was then mixed with ethidium bromide (EtBr) in cuvette. The molar ratio of the obtained EtBr to phosphate of DNA was 0.05 to minimize the possible influence of the intercalated dye on the electrostatic interaction of DNA with CSO-SA (Izumrudov et al., 2003). Equal aliquots of CSO-SA were added stepwise to the EtBr–DNA solution with stirring at 400 rpm for 5 min. The fluorescence intensity of the sample was then measured by fluoremeter (F-2500 Fluorescence spectrophotometer, Hitachi, Ltd., Japan) with the excitation and emission wavelengths of 546 nm and 600 nm, respectively. The addition of CSO-SA was end when the fluorescence intensity did not change in a wide range of N/P ratio. Data was presented as relative fluorescence intensity (Rel.FI), which was calculated by Eq. (1):

$$\text{Rel.FI}\,(\%) = \left[\frac{\text{FI}_S - \text{FI}_B}{\text{FI} - \text{FI}_B}\right] \times 100 \quad (1)$$

where FI_S, FI_B, and FI was the fluorescence intensity of sample, fluorescence intensity of blank solution and fluorescence intensity of EtBr–DNA solution, respectively.

3. Results

3.1. Synthesis and characterization of the CSO-SA

The CSO-SA with different molecular weight of CSO and SA graft ratio was synthesized by the coupling reaction of the carboxyl groups of SA and primary amino groups of CSO in the presence of EDC. The synthesis recipes and the determined amino substitute degree (SD) of CSO in the products were shown in Table 1. It was clear that SD of CSO in CSO-SA increased with increasing the charged amount of SA. From Table 1, it was also found the size of CSO-SA micelles was increased with increasing of molecular weight of CSO, and the CSO-SA with higher SD tends to own bigger micellar size. The critical micelle concentration (CMC) was also shown in Table 1. It indicated that CSO-SA with higher SD generally owned smaller CMC. The CMC of CSO-SA with approximately equal SD had no significant difference.

The pKa of synthesized CSO-SA was determined by potentiometric titration. The results were shown in Figs. 1 and 2. All titration data was fitted to Katchalsky's equation and a straight line was obtained by regression. Fig. 1 showed the potentiometric titration results of CSO-SA with CSO having 3 kDa molecular weight and different SD. Best linear relationships were obtained in the interval of log $[(1-\alpha)/\alpha]$ from −0.5 to 0.5. The similar results were found by Wang et al. (2006). As shown in Fig. 1, the pKa of CSO-SA with 9.79%, 45.01% and 63.41% SD was 8.16, 7.40 and 6.02, respectively, which decreased with the increase of SD. Similarly, the relationship between pKa and initial pH of CSO-SA aqueous solution was also found. The CSO-SA aqueous solution with higher SD had low

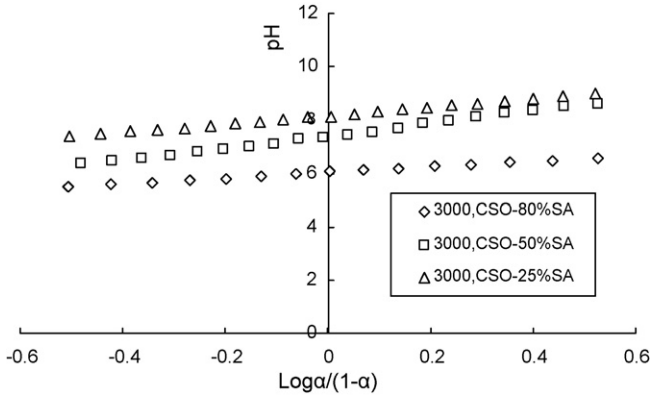

Fig. 1. Potentiometric titration data of CSO-SA aqueous solution with same molecular weight of CSO and different of substitution degree titrated by 0.01 M NaOH solution.

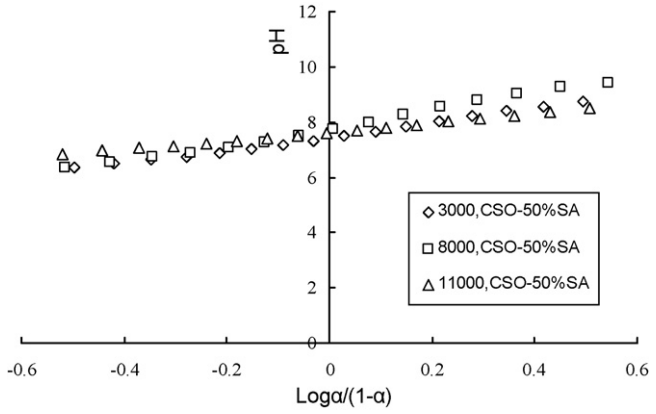

Fig. 2. Potentiometric titration data of CSO-SA aqueous solution with similar substitution degree of amino groups and different molecular weight of CSO titrated by 0.01 M NaOH solution.

pH value, which was in accordance with the reference (Sorlier et al., 2001). The initial pH of CSO-SA aqueous solution with 9.79%, 45.01% and 63.41% SD was 6.45, 5.47 and 4.95, respectively. Fig. 2 showed the potentiometric titration results of CSO-SA with CSO having different molecular weight. Here the SD of CSO-SA had the similar SD. The pKa value of CSO-SA with CSO having 18 kDa, 11 kDa and 3 kDa molecular weight was 7.80, 7.64 and 7.48, respectively.

3.2. Complexation of CSO-SA with DNA

The CSO-SA with different M_W of CSO and SD was used to prepare complexes with DNA. The N/P ratio of complexes was changed from 0.1 to 20. The size of CSO-SA/DNA complexes was determined by DLS measurement and was presented as a function of N/P ratio. Fig. 3 showed the *Z*-average diameter of complexes formed by CSO-SA having similar SD and different M_W of CSO with DNA in aqueous

Table 1
Physicochemical properties of CSO-SA with different graft ratio of stearic acid and molecular weight of CSO.

Samples	M_W (g/mol)	Theoretical SD (%)	Actual SD (%)	*Z*-average diameter (nm)	pKa value	Critical micelle concentration (μg/mL)
18000, CSO-25%SA	18,000	25.00	9.79	158.7 ± 15.8	8.432	89.6
11000, CSO-50%SA	11,000	50.00	49.46	309.4 ± 13.8	7.640	6.59
8000, CSO-50%SA	8000	50.00	47.58	202.7 ± 2.0	7.801	7.44
3000, CSO-25%SA	3000	25.00	13.88	139.0 ± 11.1	8.157	69.2
3000, CSO-50%SA	3000	50.00	45.00	143.0 ± 2.8	7.478	4.38
3000, CSO-80%SA	3000	80.00	63.41	188.1 ± 6.9	6.026	6.13
3000, CSO	3000	–	–	–	6.515	–

M_W represents in term of weight-average molecular weight of CSO. SD refers to the substitution degree of amino groups of CSO in CSO-SA.

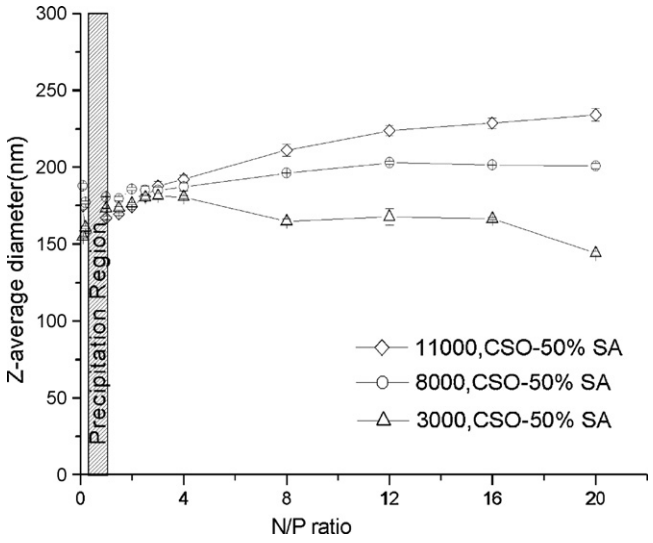

Fig. 3. *Z*-average diameters of CSO-SA/DNA complexes using CSO-SA with similar substitution degree and different molecular weight of CSO as function of N/P ratio. Data points are expressed as mean ± SD.

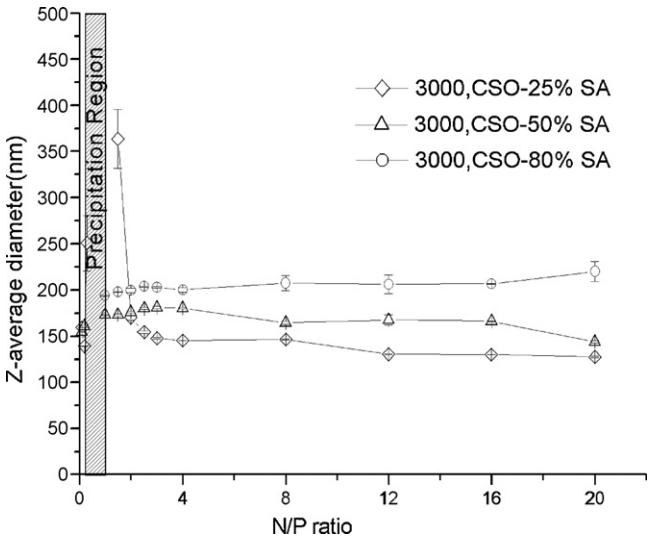

Fig. 5. *Z*-average diameters of CSO-SA/DNA complexes using CSO-SA with same molecular weight of CSO and different substitution degree of amino groups as function of N/P ratio. Data points are expressed as mean ± SD.

solution. In general, CSO-SA with higher M_W of CSO tended to form bigger complexes with DNA using the same N/P ratio. The sizes of CSO-SA/DNA complexes using CSO-SA with 11 and 8 kDa M_W of CSO increased with increasing the N/P ratio. However, in the case of CSO-SA/DNA complexes using CSO-SA with 3000 kDa M_W of CSO, the size of the complexes slightly decreased with the increase of N/P ratio, ranging from 144.0 nm to 173.3 nm. Precipitation regions for CSO-SA/DNA complexes using different molecular weight of CSO were about same. The precipitation happened when the N/P ratio was about 0.6. Zeta potentials of polyplexes were shown in Fig. 4. It was clearly demonstrated that the zeta potential of polyplexes changed from positive to negative when N/P ratio decreased from 20 to 0.5, and the absolute value of Zeta potential close to 0 as the N/P ratio near 0.8.

Fig. 5 summarized the size of complexes prepared by CSO-SA with same M_W of CSO and different SD. As can be seen from Fig. 5, the sizes of CSO-SA/DNA complexes increased with the SD of used CSO-SA. However, the sizes of CSO-SA/DNA complexes were almost constant when the N/P ratio ranged from 0.6 to 20.

Fig. 6 showed the curve of relative fluorescence intensity determined by ethidium bromide displacement assay against N/P ratio of CSO-SA/DNA complexes, in which the CSO-SA with 3 kDa M_W of CSO and different SD were used. It was found that the relative fluorescence intensity of CSO-SA/DNA complexes quenched faster when the CSO-SA with higher SD was used in the lower N/P ratio. However, in the higher N/P region, the CSO-SA/DNA complexes using CSO-SA with low SD had the low relative fluorescence intensity.

Fig. 7 showed the curve of relative fluorescence intensity against N/P ratio of CSO-SA/DNA complexes, in which the CSO-SA with the same SD and different M_w of CSO were used. It could be seen that the relative fluorescence intensity of CSO-SA/DNA complexes quenched faster when the CSO-SA with lower M_W of CSO was used.

3.3. Effect of ionic strength on complexation

Ionic strength is a key factor to affect the stability of ionic complexes. Fig. 8 showed the size change of CSO-SA/DNA complexes prepared using CSO-SA with 18 kDa M_w CSO and 9.79% SD under different N/P ratio and sodium chloride concentration. It could be seen that the complexes formed under high NaCl concentration owned big size. When the sodium chloride concentration ranged from 0.01 M to 0.1 M, no obvious change of precipitation region

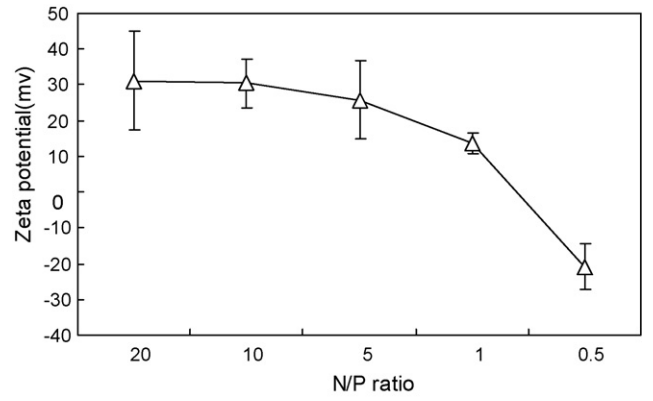

Fig. 4. Zeta potential of polyplexes with different N/P ratio. The molecular weight of CSO-SA employed in the experiments was 18 kDa and the substitution degree of SA was 9.79%. Data points are expressed as mean ± SD.

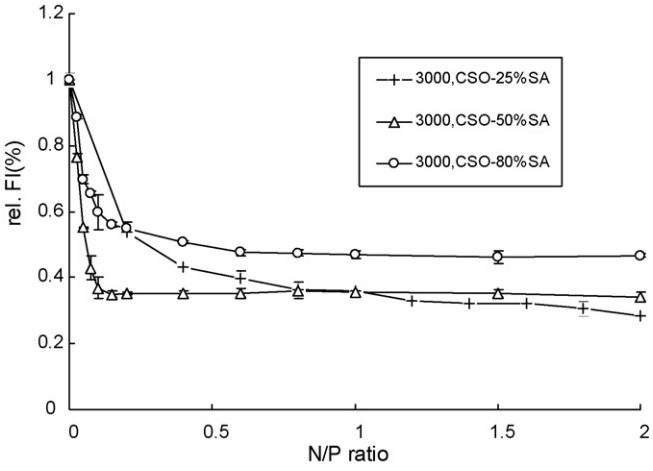

Fig. 6. Titration curves of EtBr–DNA complexes titrated by CSO-SA with same molecular weight and different substitution degree in 10 mM NaCl solution. Each sample was measured triplicate and data points are presented as mean ± SD.

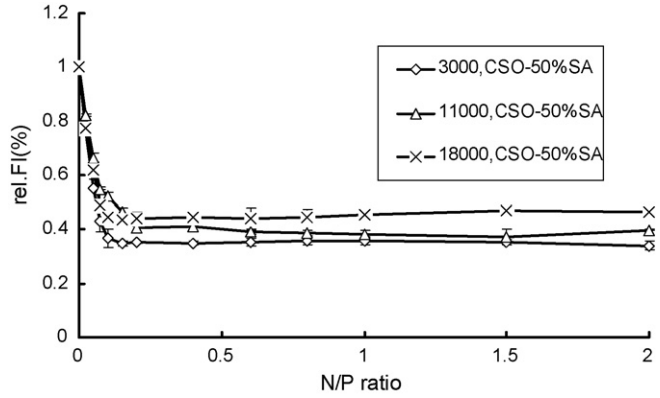

Fig. 7. Titration curves of EtBr–DNA complexes titrated by CSO-SA with similar substitution degree and different molecular weight of CSO in 10 mM NaCl solution. Each sample was measured triplicate and data points are presented as mean ± SD.

was observed. Even though, the influence of ionic strength during the formation of complexes cannot be negligible. It was found the complexes with N/P ratio 5 precipitated when the sodium chloride concentration was increase to 0.75 M. EtBr assay was further employed to confirm the influence of ionic strength on stability of complexes.

The fluorimetric titration curves of EtBr–DNA solution with CSO-SA having 18 kDa M_W CSO and 9.79% SD under different ionic strength were shown in Fig. 9. Data is presented the change of relative fluorescence intensity against N/P ratio. As expected, the addition of CSO-SA solution to EtBr–DNA solution leaded to substantial fluorescence quenching in the case of 0.01 M, 0.05 M, 0.10 M NaCl solution. The fluorescence quenched faster in the low ionic strength environment.

3.4. Effect of pH on complexation

Fig. 10 showed the size variation of CSO-SA/DNA complexes using CSO-SA having 18 kDa M_W CSO and 9.79% SD under different N/P ration and pH. As it was shown in Fig. 10, the *Z*-average diameter of complexes was affected by pH value of the environment. In general, the size of complexes was increased with the increase of N/P ratio, and the complexes prepared under pH

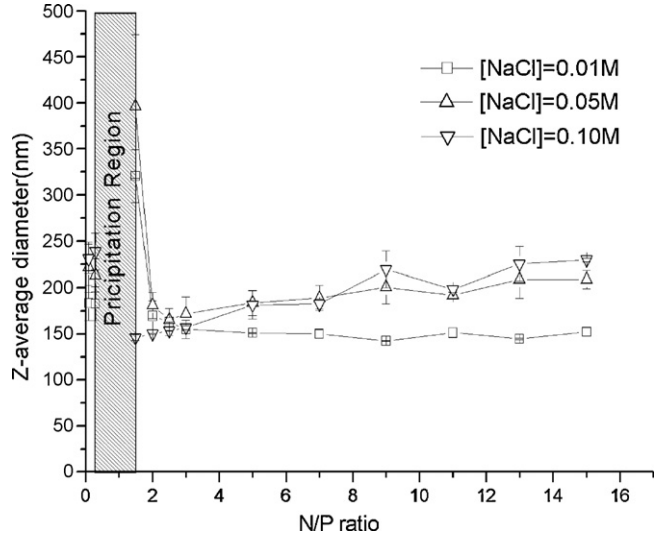

Fig. 8. *Z*-average diameters of CSO-SA/DNA complexes in different ion strength adjusted by addition of sodium chloride as a function of N/P ratio. Each sample was measured triplicate and data points are expressed as mean ± SD.

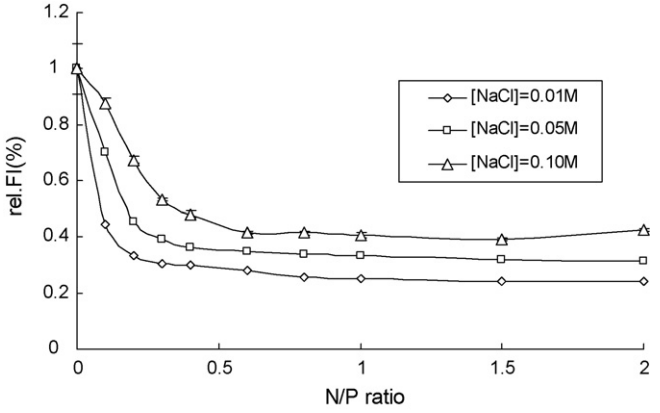

Fig. 9. Titration curves of EtBr–DNA complex titrated by CSO-SA in different ionic strength adjusted by addition of sodium chloride. Each sample was measured triplicate and data points are presented as mean ± SD.

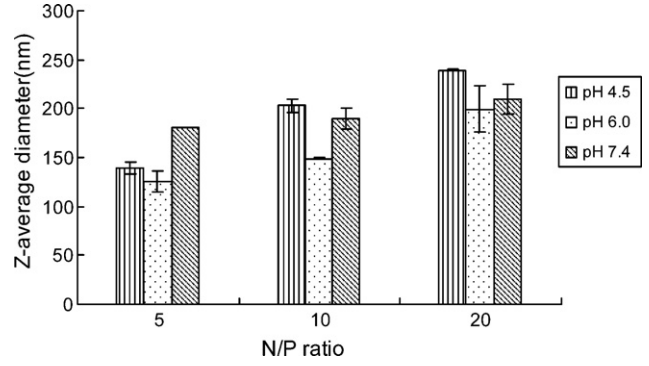

Fig. 10. *Z*-average diameters of CSO-SA/DNA complexes under different pH. The buffer solution used in this experiment was: HAc/NaAc for pH 4.5, HAc/NaAc for pH 6.0, KH_2PO_4/NaOH for pH 7.4. Each sample was measured triplicate and data points are expressed as mean ± SD.

6.0 indicated smallest size. The electrostatic interaction between CSO-SA and DNA as a function of pH, monitored by changes fluorescence intensity of EtBr–DNA solution, were shown in Fig. 11. Generally, the extent of fluorescence quenching resulting from the addition of CSO-SA was decreased with increase of pH. The complexes prepared under pH 4.5 showed most significant fluorescence quenching, compared to those prepared at pH 6.0 and 7.4.

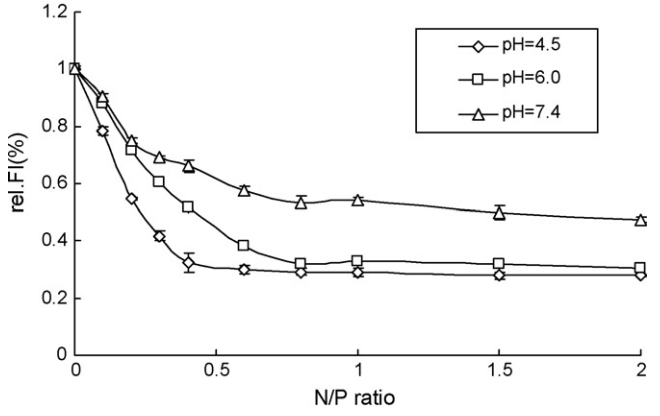

Fig. 11. Titration curves of EtBr–DNA complex titrated by CSO-SA under buffer condition with different pH value. The buffer solution used in this experiment was: HAc/NaAc for pH 4.5, HAc/NaAc for pH 6.0, KH_2PO_4/NaOH for pH 7.4. Each sample was measured triplicate and data points are presented as mean ± SD.

4. Discussion

CSO-SA is a hydrophobic modified chitosan oligosaccharide. The CSO exhibited good solubility in physiological condition and reduced cell toxicity. The CSO-SA could easily form cationic nano-sized micelles in the aqueous phase, and could be rapidly internalized into cancer cells (You et al., 2007). These essential properties were favor for gene vector (Hu et al., 2006b). The binding of CSO-SA micelles and DNA was formed by electrostatic interaction. It suggests that the charge density on the surface of CSO-SA micelles must have influence on size and stability of CSO-SA/DNA complexes. The positive charge on the surface of CSO-SA, resulting from protonation of the primary amino groups of CSO-SA, strongly depends on pKa (represents the protonation extent of amino groups) and substitution degree (reflects the proportion of primary amino groups in CSO-SA).

TNBS assay (Huang et al., 2005) was used to evaluate the proportion of primary amino groups of CSO-SA, which was widely accepted as the method in determination of primary amino groups, amine acid and protein in mixture. Primary amino groups in CSO-SA are trinitrophenylation in the reaction and the reactant had maximum UV absorbance at the wavelength of 344 nm, which is in proportion with the number of primary amino groups in CSO-SA. The data was presented in term of SD, meaning that the ratio of substituted amino groups to total primary amino groups of CSO. The actual substitution degrees of CSO-SA with different molecular weight were presented in Table 1.

Potentiometric titration was employed to determinate the pKa of CSO-SA. Actually, the ammonium form of CSO-SA can self-dissociate in the aqueous solution (Eq. (2)). The equilibrium constant of this process reflects the ability of dissociation of CSO-SA:

$$\text{CSO-SA–NH}_3 \rightarrow \text{CSO-SA–NH}_2 + \text{H}_3\text{O}^+ \quad (2)$$

$$\text{Ka} = \frac{[\text{CSO-SA–NH}_2][\text{H}_3\text{O}^+]}{[\text{CSO-SA–NH}_3{}^+]}$$

Titration data was explained by Katchalsky's equation (Eq. (3)), which was used to describe the pKa of polyelectrolytes in 1954 (Katchalsky and Spitnik, 1947). Domard (1987) first used Katchalsky's equation to evaluate the variation of pKa during the titration of chitosan (Wang et al., 2006).

$$\text{pKa} = \text{pH} + n\log\left[\frac{1-\alpha}{\alpha}\right] \quad (3)$$

In this equation, n represents the empirical parameter, which is superior to 1 in the case of chitosan. α is the degree of dissociation, which was calculated from Eq. (4):

$$\alpha = \frac{\alpha' + [\text{H}^+]}{C} \quad (4)$$

Here, α' represents the degree of neutralization, which was calculated by comparison the amount of added sodium hydroxide with the concentration of total primary amine groups in CSO-SA, $[\text{H}^+]$ was deduced from pH, and C is the total primary amino concentration in CSO-SA. A linear relationship was existed between pH and $\log[(1-\alpha)/\alpha]$ according to Katchalsky's equation, which allow us to determinate pKa from the intercept.

As it was indicated in Fig. 1, the pKa value of CSO-SA was increased with the decrease of SD, this means the primary amino groups of CSO-SA with lower SD easily protonation. However, the influence of molecular weight of CSO on pKa was not obvious. This may be due to the same proportion of primary amino groups to amino groups in CSO-SA with different molecular weight of CSO. The results are consistent with former work (Wang et al., 2006), which reported that the pKa value of chitosan showed a slightly decreasing from 6.51 to 6.39 when the molecular weight decreased from 1370 kDa to 60 kDa.

The results of size change of CSO-SA/DNA complex under different N/P ratio presented in Figs. 4 and 5 may be originated from the original size of CSO-SA micelle size. The bigger original size led the bigger size of CSO-SA/DNA complex. In the cases of CSO-SA with the same SD and 8 kDa, 11 kDa M_W of CSO, The complex size decreased with decreasing N/P ratio. The decrease in size can be explained as the formation of more compacted complex as the N/P ratio was low, because these two kinds of CSO-SA had bigger size and loose structure. In the process of complexation, precipitation region (Talelli and Pispas, 2008) was also found near N/P ratio 1, in which point the polycation available for complexation was equal to polyanion. DLS measurement data also demonstrates that in the N/P ratio closed to precipitation region, the size of complexes increased and the complexes become unstable and easy to precipitation.

Ethidium bromide (EtBr) is a cationic fluorescent probe, which intercalates between the base pairs of DNA and RNA and has large increase in fluorescence (Geall and Blagbrough, 2000; Izumrudov et al., 2002; Strand et al., 2005). The electrostatic interaction between CSO-SA and DNA results the exclusion of EtBr from DNA double helix to solution, accompanying evident decay of EtBr fluorescence. The less pronounced quenching of fluorescence means the higher fraction of EtBr remained intercalated in the DNA. Therefore, it provides an indirect way to measure the binding affinity between CSO-SA and DNA.

Fig. 6 indicated the final extent of fluorescence quenching increased with the decrease of SD, which means that CSO-SA with lower SD had higher electrostatic affinity with DNA. The variation in the affinity between CSO-SA with different SD may point toward the difference in surface density on the CSO-SA. This result was consistent with the pKa data of CSO-SA. CSO-SA with higher surface charge density had higher electrostatic affinity with DNA. In the cases of using CSO-SA with same SD and different M_W of CSO (Fig. 7), the fluorescence quenching rate was slightly increased with decreasing M_W of CSO in CSO-SA. The result means the CSO-SA with low M_W of CSO easily bind with DNA

Since CSO-SA and DNA bind to each other via electrostatic interaction, it is therefore to be believed that ionic strength has impact on the complexation via affecting the charge density of both CSO-SA and DNA. The complex size in Fig. 8 showed the substantial size increase as the ionic strength increasing from 0.01 M to 0.10 M. The increase of complexes size is associated to the reduction of electrostatic affinity between CSO-SA and DNA, resulting more loose structure was formed. The salt decreases the electrostatics interaction between CSO-SA and DNA, handicapping the displacement of EtBr from EtBr–DNA complexes by the addition of CSO-SA (Fig. 9). It can be concluded that high salt concentration facilitates the dissociation of CSO-SA/DNA complexes, making the complexes unstable and easy to precipitation. The decrease of electrostatic interaction can be explained by electrostatics shielding of the charge through formation of ion pairs (Kim et al., 2003).

As demonstrated in Eq. (2), the protonation of the primary amino groups in CSO-SA is also impacted by pH value of the aqueous solution. The low pH value may facilitate the protonation process, increasing the charge density on the surface of micelles, therefore increasing the electrostatic affinity between CSO-SA and DNA (Fig. 11).

5. Conclusions

The chemical conjugate of CSO-SA could form cationic micelle with nano-size by self-assembly. The cationic CSO-SA micelles could complex with DNA via electrostatic interaction. The pKa of

CSO-SA mainly depended on the graft ratio of SA. The lower graft ratio of SA led the higher pKa of CSO-SA. The lower graft ratio of SA and molecular weight of CSO favored the binding of CSO-SA and DNA, improving the stability of CSO-SA/DNA complex. The ionic strength and pH also affected the complexation of CSO-SA with DNA. The low ionic strength and pH favored the formation of stable CSO-SA/DNA complex.

Acknowledgements

We appreciate the financial support of the National Nature Science Foundation of China under Contract 30873174 and the Nature Science Foundation of Zhejiang province under Contract z207489.

References

Dokka, S., Toledo, D., Shi, X., Ye, Y., Rojanasakul, Y., 2000. High-efficiency gene transfection of macrophages by lipoplexes. Int. J. Pharm. 206, 97–104.

Domard, A., 1987. pH and c.d. measurements on a fully deacetylated chitosan: application to CuII–polymer interactions. Int. J. Biol. Macromol. 9, 98–104.

Geall, A.J., Blagbrough, I.S., 2000. Rapid and sensitive ethidium bromide fluorescence quenching assay of polyamine conjugate–DNA interactions for the analysis of lipoplex formation in gene therapy. J. Pharm. Biomed. Anal. 22, 849–859.

Geall, A.J., Eaton, M.A.W., Baker, T., Catterall, C., Blagbrough, I.S., 1999. The regiochemical distribution of positive charges along cholesterol polyamine carbamates plays significant roles in modulating DNA binding affinity and lipofection. FEBS Lett. 459, 337–342.

Hu, F.Q., Li, Y.H., Yuan, H., Zeng, S., 2006a. Novel self-aggregates of chitosan oligosaccharide grafted stearic acid: preparation, characterization and protein association. Pharmazie 61, 188–193.

Hu, F.Q., Zhao, M.D., Yuan, H., You, J., Du, Y.Z., Zeng, S., 2006b. A novel chitosan oligosaccharide–stearic acid micelles for gene delivery: properties and in vitro transfection studies. Int. J. Pharm. 315, 158–166.

Huang, M., Fong, C.W., Khor, E., Lim, L.Y., 2005. Transfection efficiency of chitosan vectors: effect of polymer molecular weight and degree of deacetylation. J. Control. Release 106, 391–406.

Izumrudov, V.A., Wahlund, P.O., Gustavsson, P.E., Larsson, P.O., Galaev, I.Y., 2003. Factors controlling phase separation in water–salt solutions of DNA and polycations. Langmuir 19, 4733–4739.

Izumrudov, V.A., Zhiryakova, M.V., Goulko, A.A., 2002. Ethidium bromide as a promising probe for studying DNA interaction with cationic amphiphiles and stability of the resulting complexes. Langmuir 18, 10348–10356.

Jiang, H.L., Kim, Y.K., Arote, R., Nah, J.W., Cho, M.H., Choi, Y.J., Akaike, T., Cho, C.S., 2007. Chitosan-graft-polyethylenimine as a gene carrier. J. Control. Release 117, 273–280.

Katchalsky, A., Spitnik, P., 1947. Potentiometric titrations of polymethacrylic acid. J. Polym. Sci. 12, 159–184.

Kim, T., Bai, C.Z., Nam, K., Park, J., 2009. Comparison between arginine conjugated PAMAM dendrimers with structural diversity for gene delivery systems. J. Control. Release 136, 132–139.

Kim, T.H., Ihm, J.E., Choi, Y.J., Nah, J.W., Cho, C.S., 2003. Efficient gene delivery by urocanic acid-modified chitosan. J. Control. Release 93, 389–402.

Kim, T.H., Jiang, H.L., Jere, D., Park, I.K., Cho, M.H., Nah, J.W., Choi, Y.J., Akaike, T., Cho, C.S., 2007. Chemical modification of chitosan as a gene carrier in vitro and in vivo. Prog. Polym. Sci. 32, 726–753.

Köping-Höggård, M., Vårum, K.M., Issa, M., Danielsen, S., Christensen, B.E., Stokke, B.T., Artursson, P., 2004. Improved chitosan-mediated gene delivery based on easily dissociated chitosan polyplexes of highly defined chitosan oligomers. Gene Ther. 11, 1441–1452.

Lee, K.Y., Kwon, I.C., Kim, Y.H., Jo, W.H., Jeong, S.Y., 1998. Preparation of chitosan self-aggregates as a gene delivery system. J. Control. Release 51, 213–220.

Liu, W.G., Yao, K.D., 2002. Chitosan and its derivatives—a promising non-viral vector for gene transfection. J. Control. Release 83, 1–11.

MacLaughlin, F.C., Mumper, R.J., Wang, J., Tagliaferri, J.M., Gill, I., Hinchcliffe, M., Rolland, A.P., 1998. Chitosan and depolymerized chitosan oligomers as condensing carriers for in vivo plasmid delivery. J. Control. Release 56, 259–272.

Mansouri, S., Lavigne, P., Corsi, K., Benderdour, M., Beaumont, E., Fernandes, J.C., 2004. Chitosan–DNA nanoparticles as non-viral vectors in gene therapy: strategies to improve transfection efficacy. Eur. J. Pharm. Biopharm. 57, 1–8.

Prabha, S., Zhou, W.Z., Panyam, J., Labhasetwar, V., 2002. Size-dependency of nanoparticle-mediated gene transfection: studies with fractionated nanoparticles. Int. J. Pharm. 244, 105–115.

Richardson, S.C.W., Kolbe, H.V.J., Duncan, R., 1999. Potential of low molecular mass chitosan as a DNA delivery system: biocompatibility, body distribution and ability to complexes and protect DNA. Int. J. Pharm. 178, 231–243.

Sorlier, P., Denuzière, A., Viton, C., Domard, A., 2001. Relation between the degree of acetylation and the electrostatic properties of chitin and chitosan. Biomacromolecules 2, 765–772.

Strand, S.P., Danielsen, S., Christensen, B.E., Vårum, K.M., 2005. Influence of chitosan structure on the formation and stability of DNA–chitosan polyelectrolyte complexes. Biomacromolecules 6, 3357–3366.

Talelli, M., Pispas, S., 2008. Complexes of cationic block copolymer micelles with DNA: histone/DNA complex mimetics. Macromol. Biosci. 8, 960–967.

Wang, Q.Z., Chen, X.G., Liu, N., Wang, S.X., Liu, C.S., Meng, X.H., Liu, C.G., 2006. Protonation constants of chitosan with different molecular weight and degree of deacetylation. Carbohydr. Polym. 65, 194–201.

Wasungu, L., Hoekstra, D., 2006. Cationic lipids, lipoplexes and intracellular delivery of genes. J. Control. Release 116, 255–264.

Wetering, P., Cherng, J.Y., Talsma, H., Hennink, W.E., 1997. Relation between transfection efficiency and cytotoxicity of poly (2-(dimethylamino) ethyl methacrylate)/plasmid complexes. J. Control. Release 49, 59–69.

You, J., Hu, F.Q., Du, Y.Z., Yuan, H., Ye, B.F., 2007. High cytotoxicity and resistant-cell reversal of novel paclitaxel loaded micelles by enhancing the molecular-target delivery of the drug. Nanotechnology 18, 495101.

Zhang, L., Nguyen, T.L.U., Bernard, J., Davis, T.P., Kowollik, B.K., Stenzel, M.H., 2007. Shell-cross-linked micelles containing cationic polymers synthesized via the RAFT process: toward a more biocompatible gene delivery system. Biomacromolecules 8, 2890–2901.